CHAPTER

17

COMPRESSIBLE FLOW

2022 Fall semester

Objectives

- Develop the general relations for compressible flows encountered when gases flow at high speeds.
- Introduce the concepts of stagnation state, speed of sound, and Mach number for a compressible fluid.
- Develop the relationships between the static and stagnation fluid properties for isentropic flows of ideal gases.
- Derive the relationships between the static and stagnation fluid properties as functions of specific-heat ratios and Mach number.
- Derive the effects of area changes for one-dimensional isentropic subsonic and supersonic flows.
- Solve problems of isentropic flow through converging and converging–diverging nozzles.
- Discuss the shock wave and the variation of flow properties across the shock wave.
- Develop the concept of duct flow with heat transfer and negligible friction known as Rayleigh flow.
- Examine the operation of steam nozzles commonly used in steam turbines.

17-1 STAGNATION PROPERTIES

Stagnation (or **total**) **enthalpy**

$$h_0 = h + \frac{V^2}{2} \qquad \text{(kJ/kg)}$$

Static enthalpy: the ordinary enthalpy h

Energy balance (with no heat or work interaction, no change in potential energy):

$$h_1 + \frac{V_1^2}{2} = h_2 + \frac{V_2^2}{2} \quad \rightarrow \quad h_{01} = h_{02}$$

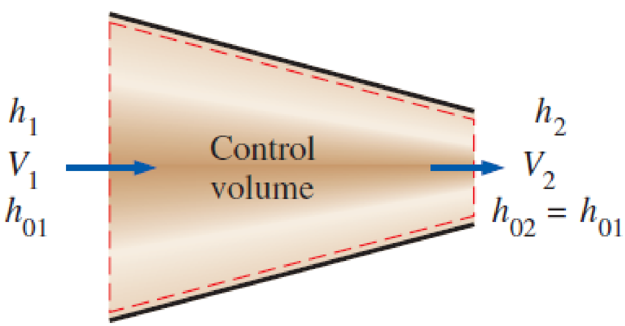

FIGURE 17–2
Steady flow of a fluid through an adiabatic duct.

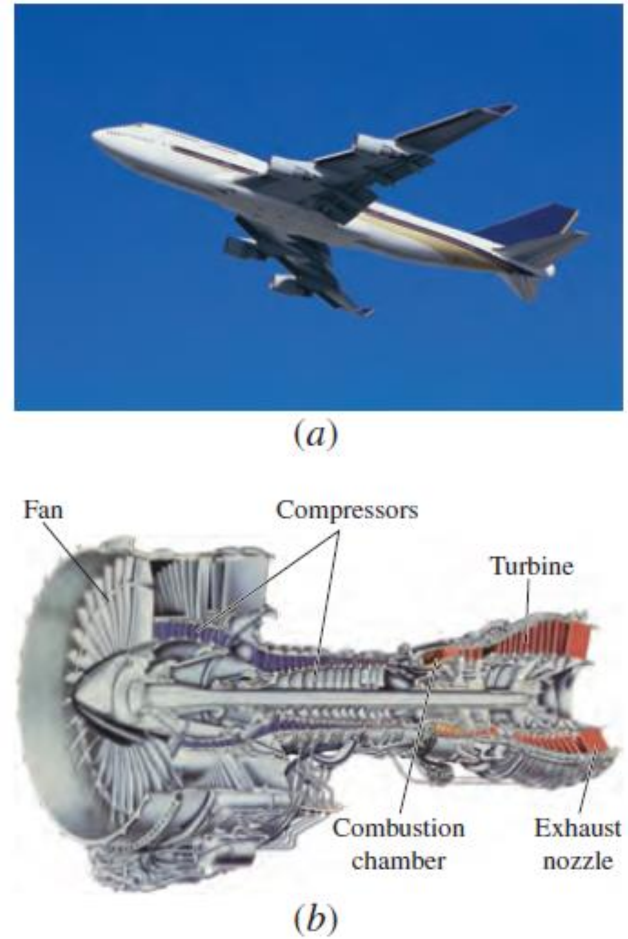

FIGURE 17–1
Aircraft and jet engines involve high speeds, and thus the kinetic energy term should always be considered when analyzing them.

17-1 STAGNATION PROPERTIES

If the fluid were brought to a complete stop, the energy balance becomes:

$$h_1 + \frac{V_1^2}{2} = h_2 = h_{02}$$

Stagnation enthalpy: The enthalpy of a fluid when it is brought to rest adiabatically.

During a stagnation process, the kinetic energy of a fluid is converted to enthalpy, which results in an increase in the fluid temperature and pressure.

The properties of a fluid at the stagnation state are called **stagnation properties** (stagnation temperature, stagnation pressure, stagnation density, etc.).

The stagnation state is indicated by the subscript 0.

17-1 STAGNATION PROPERTIES

Isentropic stagnation state: When the stagnation process is reversible as well as adiabatic (i.e., isentropic).

The stagnation processes are often approximated to be isentropic, and the isentropic stagnation properties are simply referred to as stagnation properties.

When the fluid is approximated as an *ideal gas* with constant specific heats

$$c_p T_0 = c_p T + \frac{V^2}{2} \rightarrow T_0 = T + \frac{V^2}{2c_p}$$

T_0 is called the **stagnation** (or **total**) **temperature**, and it represents *the temperature an ideal gas attains when it is brought to rest adiabatically.*

The term $V^2/2c_p$ corresponds to the temperature rise during such a process and is called the **dynamic temperature**.

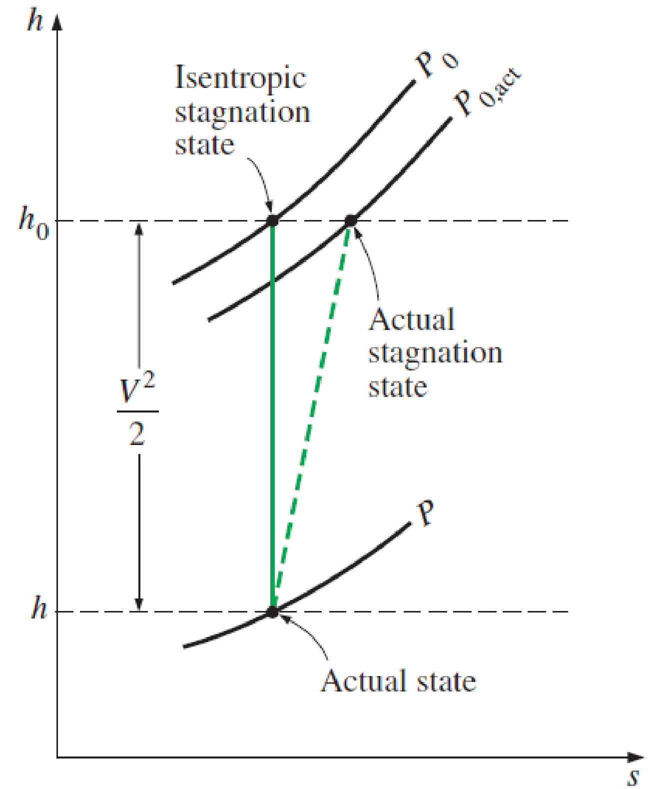

FIGURE 17–3

The actual state, actual stagnation state, and isentropic stagnation state of a fluid on an *h*-*s* diagram.

17-1 STAGNATION PROPERTIES

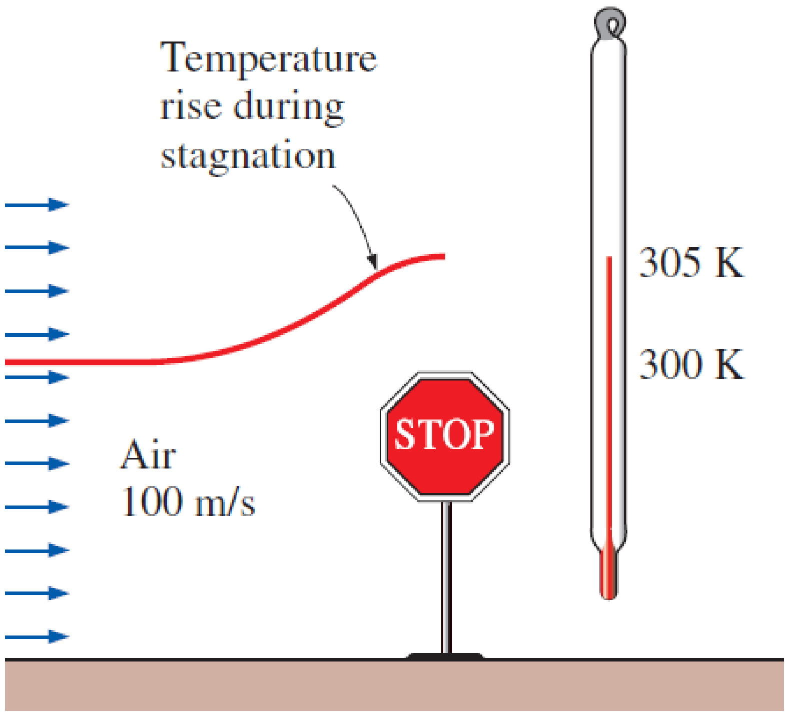

FIGURE 17–4

The temperature of an ideal gas flowing at a velocity V rises by $V^2/2c_p$ when it is brought to a complete stop.

The pressure a fluid attains when brought to rest isentropically is called the **stagnation pressure** P_0.

$$\frac{P_0}{P} = \left(\frac{T_0}{T}\right)^{k/(k-1)}$$

Stagnation density ρ_0

$$\rho = 1/v$$

$$Pv^k = P_0 v_0^k$$

$$\rightarrow \quad \frac{\rho_0}{\rho} = \left(\frac{T_0}{T}\right)^{1/(k-1)}$$

When stagnation enthalpies are used, the energy balance for a single-stream, steady-flow device

$$\dot{E}_{\text{in}} = \dot{E}_{\text{out}}$$

$$q_{\text{in}} + w_{\text{in}} + (h_{01} + gz_1) = q_{\text{out}} + w_{\text{out}} + (h_{02} + gz_2)$$

When the fluid is approximated as an *ideal gas* with constant specific heats

$$(q_{\text{in}} - q_{\text{out}}) + (w_{\text{in}} - w_{\text{out}}) = c_p(T_{02} - T_{01}) + g(z_2 - z_1)$$

Speed of sound (or the **sonic speed**): The speed at which an infinitesimally small pressure wave travels through a medium.

To obtain a relation for the speed of sound in a medium, the systems in the figures are considered.

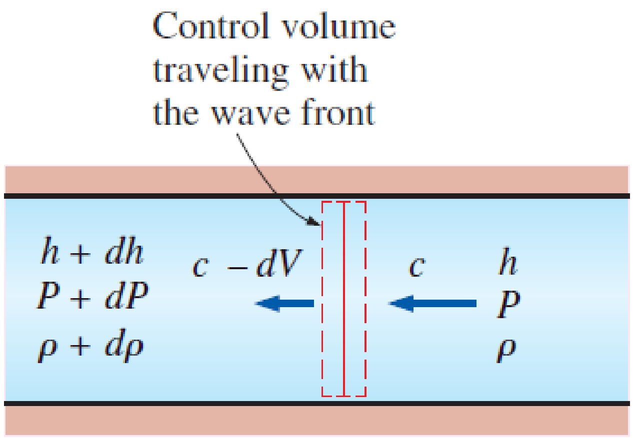

FIGURE 17–7
Control volume moving with the small pressure wave along a duct.

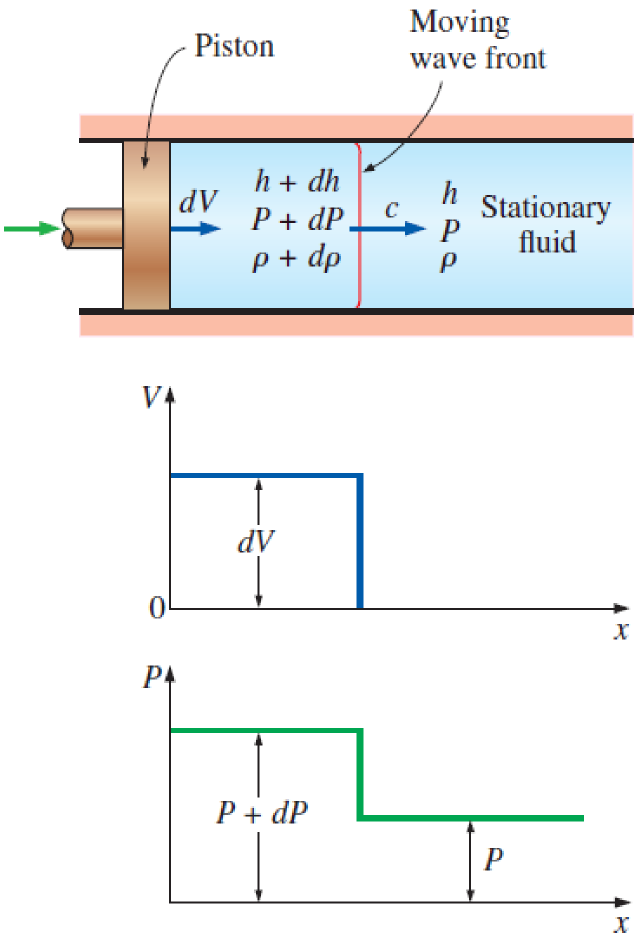

FIGURE 17–6
Propagation of a small pressure wave along a duct.

17-2 SPEED OF SOUND AND MACH NUMBER

$$c^2 = k\left(\frac{\partial P}{\partial \rho}\right)_T$$ Speed of sound

For an ideal gas $P = \rho RT$

$$c^2 = k\left(\frac{\partial P}{\partial \rho}\right)_T = k\left[\frac{\partial(\rho RT)}{\partial \rho}\right]_T = kRT$$

$$c = \sqrt{kRT}$$

$$\text{Ma} = \frac{V}{c}$$ Mach number

Ma = 1 Sonic flow
Ma < 1 Subsonic flow
Ma > 1 Supersonic flow
Ma >> 1 Hypersonic flow
Ma ≅ 1 Transonic flow

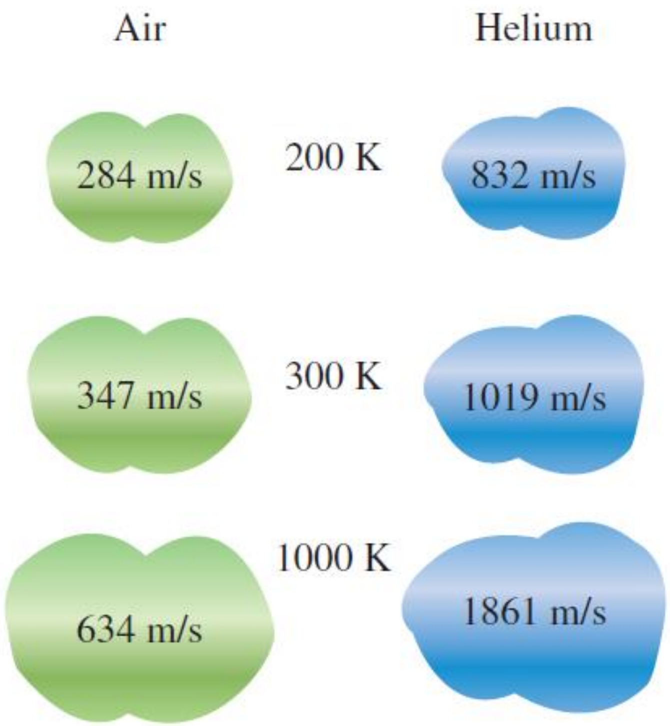

FIGURE 17–9
The speed of sound changes with temperature and varies with the fluid.

FIGURE 17–10
The Mach number can be different at different temperatures even if the flight speed is the same.

FIGURE 17–8

The speed of sound in air increases with temperature. At typical outside temperatures, c is about 340 m/s. In round numbers, therefore, the sound of thunder from a lightning strike travels about 1 km in 3 seconds. If you see the lightning and then hear the thunder less than 3 seconds later, you know that the place where the lightning occurred is less than 1 km away.

17-3 ONE-DIMENSIONAL ISENTROPIC FLOW

During fluid flow through many devices such as nozzles, diffusers, and turbine blade passages, flow quantities vary primarily in the flow direction only, and the flow can be approximated as one-dimensional isentropic flow with good accuracy.

EXAMPLE

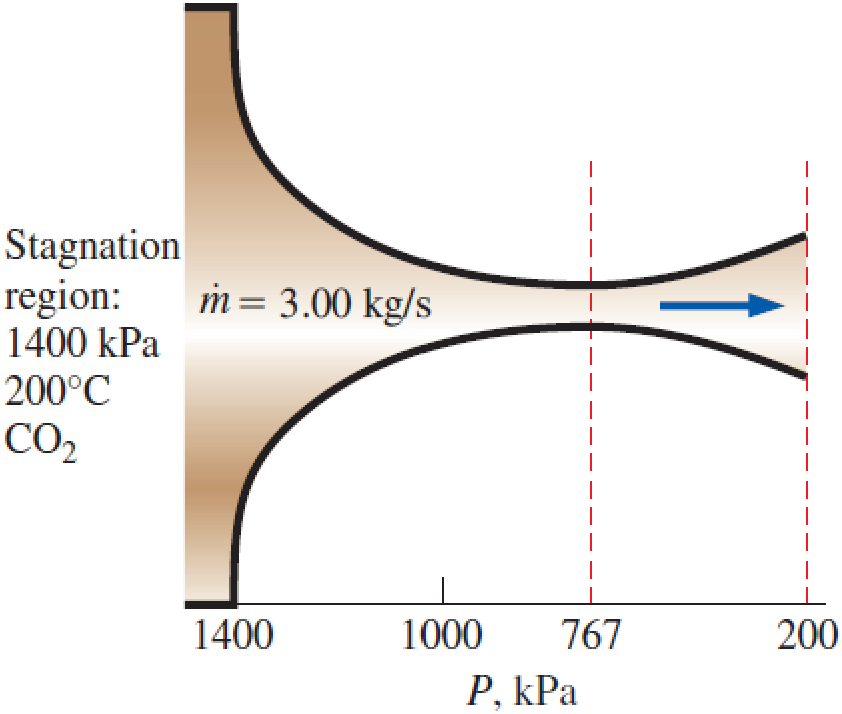

A converging–diverging nozzle.

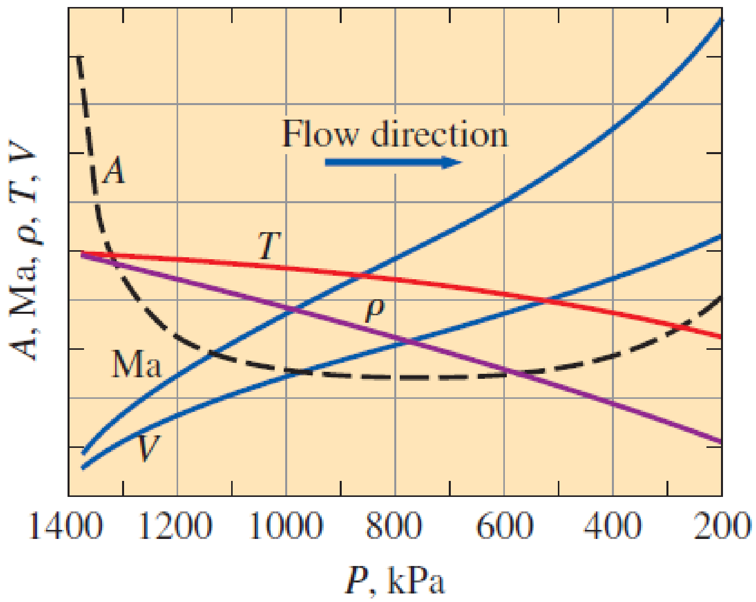

FIGURE 17–13
Variation of normalized fluid properties and cross-sectional area along a duct as the pressure drops from 1400 to 200 kPa.

TABLE 17–1

Variation of fluid properties in flow direction in the duct described in Example 17–3 for $\dot{m}$ = 3 kg/s = constant

P, kPa	T, K	V, m/s	ρ, kg/m^3	c, m/s	A, cm^2	Ma
1400	473	0	15.7	339.4	∞	0
1200	457	164.5	13.9	333.6	13.1	0.493
1000	439	240.7	12.1	326.9	10.3	0.736
800	417	306.6	10.1	318.8	9.64	0.962
767*	413	317.2	9.82	317.2	9.63	1.000
600	391	371.4	8.12	308.7	10.0	1.203
400	357	441.9	5.93	295.0	11.5	1.498
200	306	530.9	3.46	272.9	16.3	1.946

* 767 kPa is the critical pressure where the local Mach number is unity.

17-3 ONE-DIMENSIONAL ISENTROPIC FLOW

We note from Example that the flow area decreases with decreasing pressure up to a critical-pressure value (Ma = 1), and then it begins to increase with further reductions in pressure.

The Mach number is unity at the location of smallest flow area, called the **throat**.

The velocity of the fluid keeps increasing after passing the throat although the flow area increases rapidly in that region.

This increase in velocity past the throat is due to the rapid decrease in the fluid density.

The flow area of the duct considered in this example first decreases and then increases. Such ducts are called **converging–diverging nozzles**.

These nozzles are used to accelerate gases to supersonic speeds and should not be confused with *Venturi nozzles*, which are used strictly for incompressible flow.

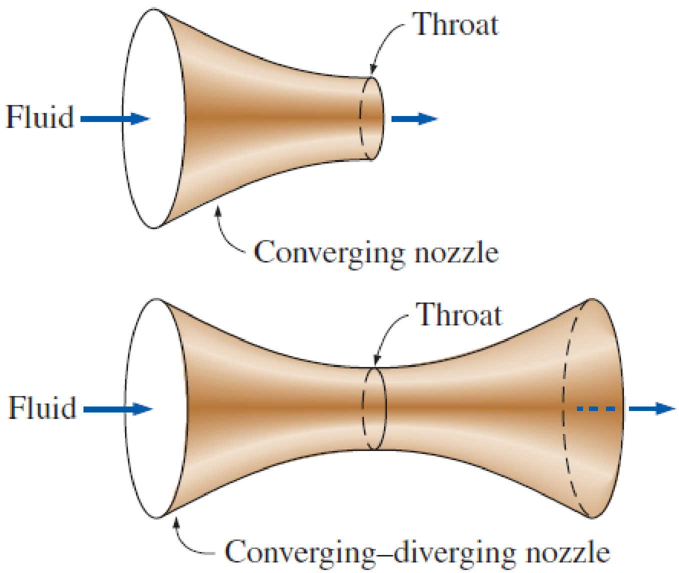

FIGURE 17–14
The cross section of a nozzle at the smallest flow area is called the *throat*.

Variation of Fluid Velocity with Flow Area

In this section, the relations for the variation of static-to-stagnation property ratios with the Mach number for pressure, temperature, and density are provided.

$$\frac{dA}{A} = \frac{dP}{\rho V^2}(1 - \mathrm{Ma}^2)$$

This relation describes the variation of pressure with flow area.

At subsonic velocities, the pressure decreases in converging ducts (subsonic nozzles) and increases in diverging ducts (subsonic diffusers).

At supersonic velocities, the pressure decreases in diverging ducts (supersonic nozzles) and increases in converging ducts (supersonic diffusers).

CONSERVATION OF ENERGY
(steady flow, $w = 0$, $q = 0$, $\Delta\mathrm{pe} = 0$)

$$h_1 + \frac{V_1^2}{2} = h_2 + \frac{V_2^2}{2}$$

or

$$h + \frac{V^2}{2} = \text{constant}$$

Differentiate,

$$dh + V\,dV = 0$$

Also,

$$T\,\cancelto{0 \text{ (isentropic)}}{ds} = dh - v\,dP$$

$$dh = v\,dP = \frac{1}{\rho}\,dP$$

Substitute,

$$\frac{dP}{\rho} + V\,dV = 0$$

FIGURE 17–15
Derivation of the differential form of the energy equation for steady isentropic flow.

17-3 ONE-DIMENSIONAL ISENTROPIC FLOW

$$\frac{dA}{A} = -\frac{dV}{V}(1 - \mathrm{Ma}^2)$$

This equation governs the shape of a nozzle or a diffuser in subsonic or supersonic isentropic flow.

For subsonic flow ($\mathrm{Ma} < 1$), $\frac{dA}{dV} < 0$

For supersonic flow ($\mathrm{Ma} > 1$), $\frac{dA}{dV} > 0$

For sonic flow ($\mathrm{Ma} = 1$), $\frac{dA}{dV} = 0$

The proper shape of a nozzle depends on the highest velocity desired relative to the sonic velocity.

To accelerate a fluid, we must use a converging nozzle at subsonic velocities and a diverging nozzle at supersonic velocities.

To accelerate a fluid to supersonic velocities, we must use a converging–diverging nozzle.

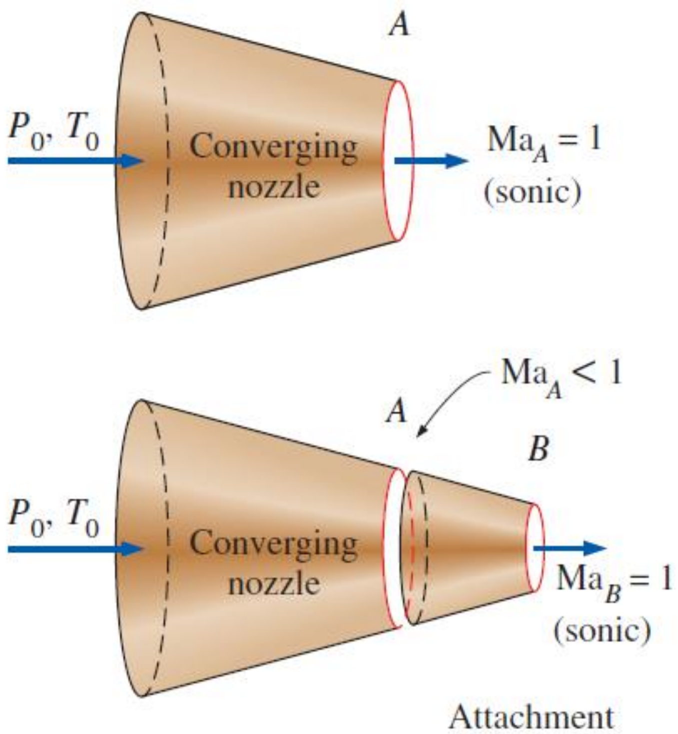

FIGURE 17–16
We cannot attain supersonic velocities by extending the converging section of a converging nozzle. Doing so will only move the sonic cross section farther downstream and decrease the mass flow rate.

17-3 ONE-DIMENSIONAL ISENTROPIC FLOW

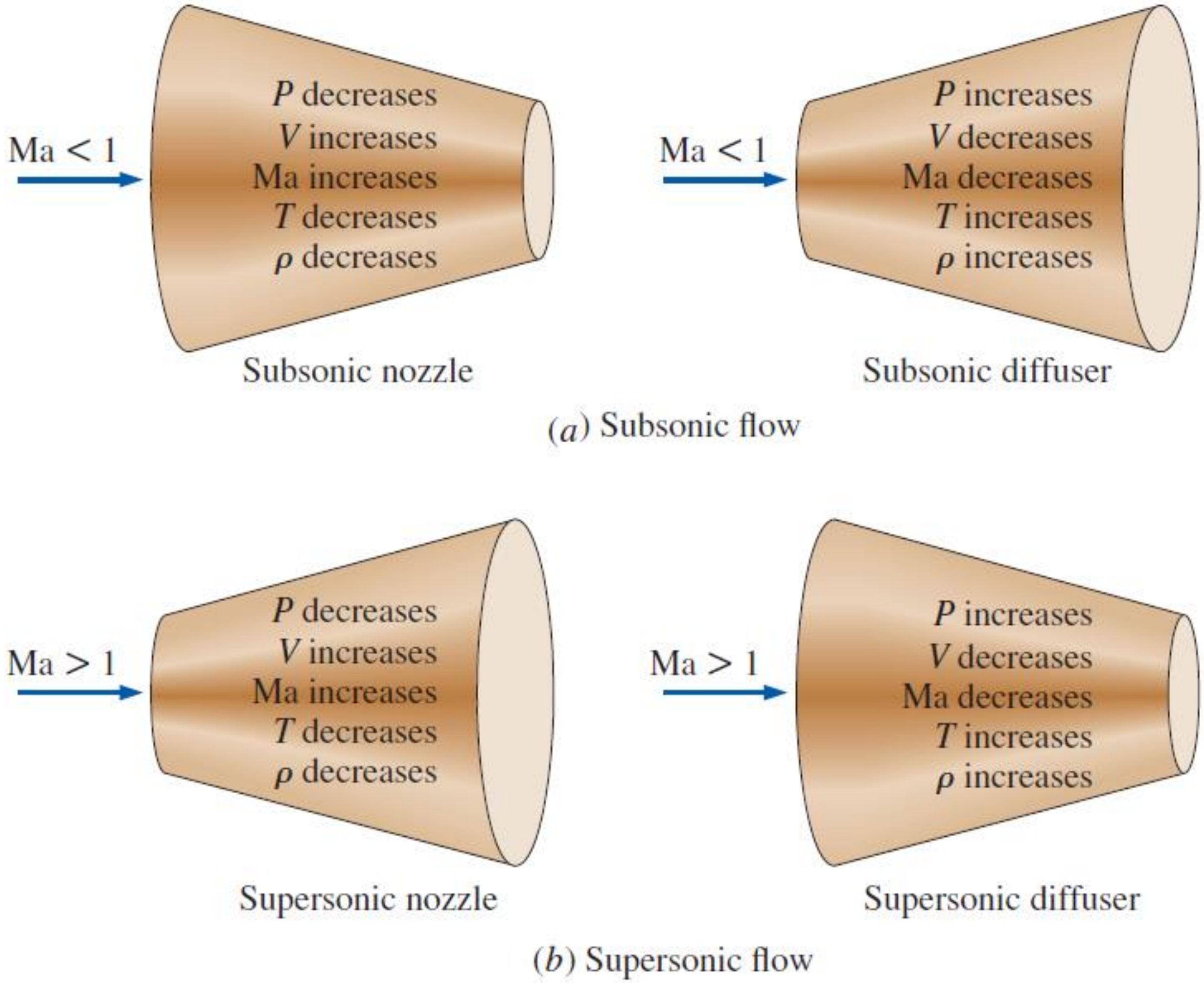

FIGURE 17–17
Variation of flow properties in subsonic and supersonic nozzles and diffusers.

Property Relations for Isentropic Flow of Ideal Gases

The relations between the static properties and stagnation properties of an ideal gas with constant specific heats

$$\frac{T_0}{T} = 1 + \left(\frac{k-1}{2}\right)\text{Ma}^2$$

$$\frac{P_0}{P} = \left[1 + \left(\frac{k-1}{2}\right)\text{Ma}^2\right]^{k/(k-1)}$$

$$\frac{\rho_0}{\rho} = \left[1 + \left(\frac{k-1}{2}\right)\text{Ma}^2\right]^{1/(k-1)}$$

$$\frac{T^*}{T_0} = \frac{2}{k+1}$$

$$\frac{P^*}{P_0} = \left(\frac{2}{k+1}\right)^{k/(k-1)}$$

$$\frac{\rho^*}{\rho_0} = \left(\frac{2}{k+1}\right)^{1/(k-1)}$$

Critical ratios (Ma=1)

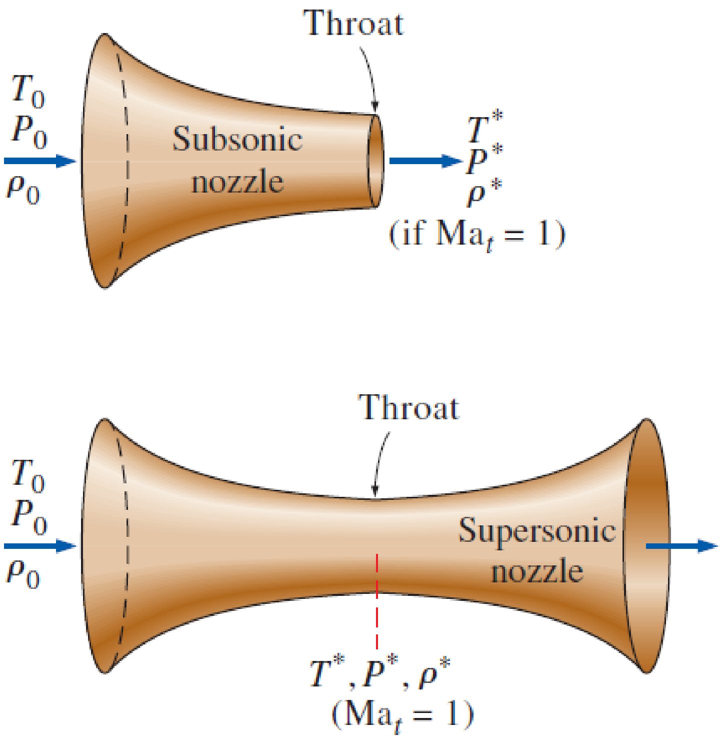

FIGURE 17–18
When $\text{Ma}_t = 1$, the properties at the nozzle throat are the critical properties.

17-3 ONE-DIMENSIONAL ISENTROPIC FLOW

TABLE 17–2

The critical-pressure, critical-temperature, and critical-density ratios for isentropic flow of some ideal gases

	Superheated steam, $k = 1.3$	Hot products of combustion, $k = 1.33$	Air, $k = 1.4$	Monatomic gases, $k = 1.667$
$\frac{P^*}{P_0}$	0.5457	0.5404	0.5283	0.4871
$\frac{T^*}{T_0}$	0.8696	0.8584	0.8333	0.7499
$\frac{\rho^*}{\rho_0}$	0.6276	0.6295	0.6340	0.6495

Converging or converging–diverging nozzles are found in steam and gas turbines and aircraft and spacecraft propulsion systems.

In this section we consider the effects of **back pressure** (i.e., the pressure applied at the nozzle discharge region) on the exit velocity, the mass flow rate, and the pressure distribution along the nozzle.

Converging Nozzles

Mass flow rate through a nozzle

$$\dot{m} = \frac{A\text{Ma}P_0\sqrt{k/(RT_0)}}{[1 + (k - 1)\text{Ma}^2/2]^{(k+1)/[2(k-1)]}}$$

Maximum mass flow rate

$$\dot{m}_{max} = A^*P_0\sqrt{\frac{k}{RT_0}}\left(\frac{2}{k + 1}\right)^{(k+1)/[2(k-1)]}$$

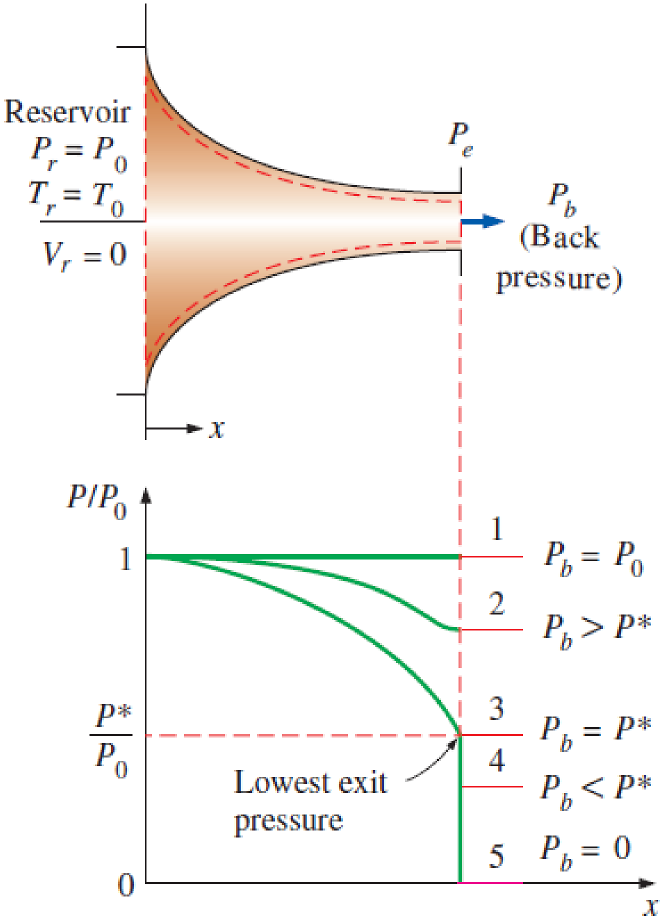

FIGURE 17–20
The effect of back pressure on the pressure distribution along a converging nozzle.

$$P_e = \begin{cases} P_b & \text{for } P_b \geq P^* \\ P^* & \text{for } P_b < P^* \end{cases}$$

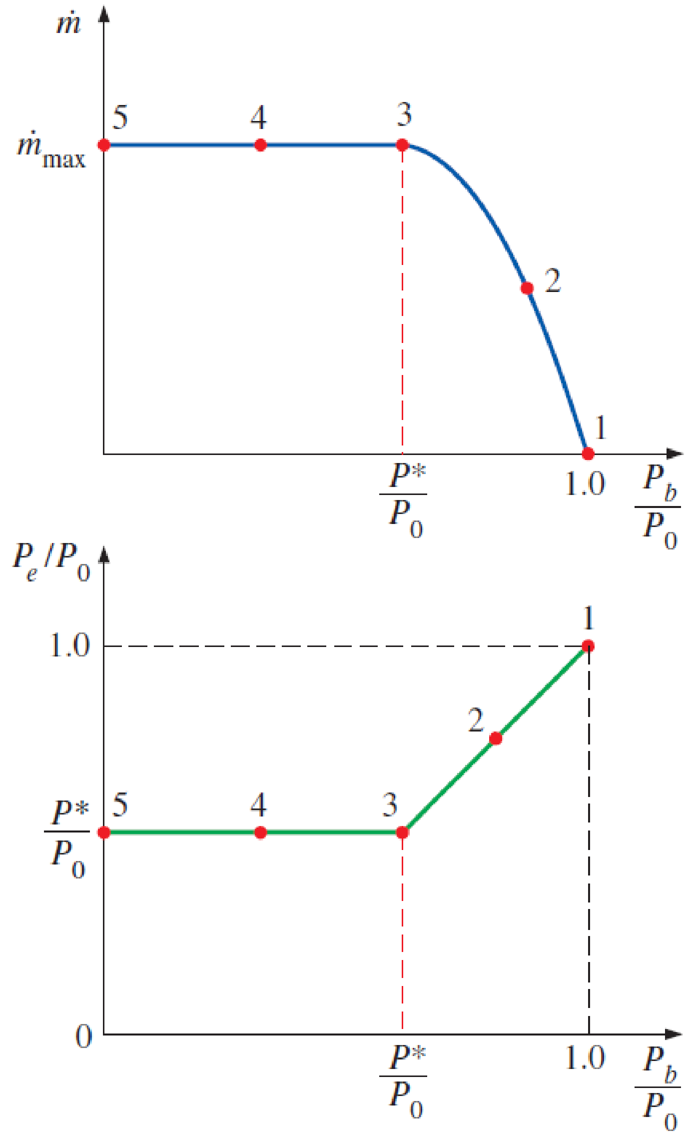

FIGURE 17–21

The effect of back pressure P_b on the mass flow rate $\dot{m}$ and the exit pressure P_e of a converging nozzle.

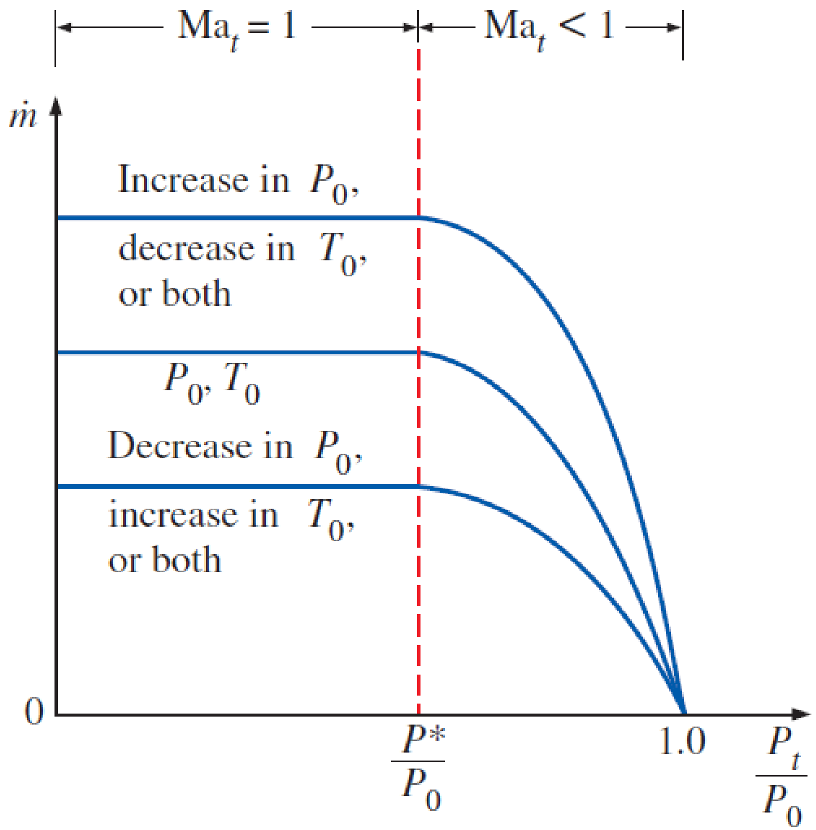

FIGURE 17–22

The variation of the mass flow rate through a nozzle with inlet stagnation properties.

17-4. ISENTROPIC FLOW THROUGH NOZZLES

$$\frac{A}{A^*} = \frac{1}{\text{Ma}}\left[\left(\frac{2}{k+1}\right)\left(1+\frac{k-1}{2}\text{Ma}^2\right)\right]^{(k+1)/[2(k-1)]}$$

$$\text{Ma}^* = \frac{V}{c^*} \qquad \text{Ma}^* = \frac{V}{c}\frac{c}{c^*} = \frac{\text{Ma}\,c}{c^*} = \frac{\text{Ma}\sqrt{kRT}}{\sqrt{kRT^*}} = \text{Ma}\sqrt{\frac{T}{T^*}}$$

$$\text{Ma}^* = \text{Ma}\sqrt{\frac{k+1}{2+(k-1)\text{Ma}^2}}$$

Ma* is the local velocity nondimensionalized with respect to the sonic velocity at the *throat*.

Ma is the local velocity nondimensionalized with respect to the *local* sonic velocity.

Ma	Ma^*	$\frac{A}{A^*}$	$\frac{P}{P_0}$	$\frac{\rho}{\rho_0}$	$\frac{T}{T_0}$
⋮	⋮	⋮	⋮	⋮	⋮
0.90	0.9146	1.0089	0.5913	⋮	⋮
1.00	1.0000	1.0000	0.5283	⋮	⋮
1.10	1.0812	1.0079	0.4684	⋮	⋮
⋮	⋮	⋮	⋮	⋮	⋮

FIGURE 17–23
Various property ratios for isentropic flow through nozzles and diffusers are listed in Table A–32 for $k = 1.4$ (air) for convenience.

Converging–Diverging Nozzles

The highest velocity in a converging nozzle is limited to the sonic velocity (Ma = 1), which occurs at the exit plane (throat) of the nozzle.

Accelerating a fluid to supersonic velocities (Ma > 1) can be accomplished only by attaching a diverging flow section to the subsonic nozzle at the throat (a converging–diverging nozzle), which is standard equipment in supersonic aircraft and rocket propulsion.

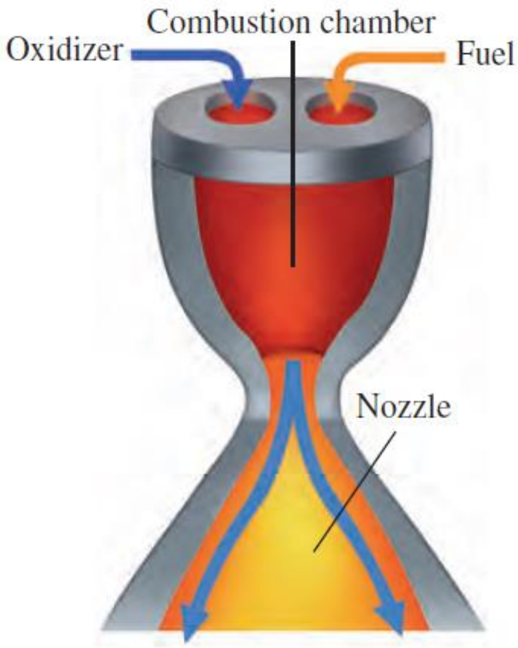

FIGURE 17–26
Converging–diverging nozzles are commonly used in rocket engines to provide high thrust.

When $P_b = P_0$ (case A), there will be no flow through the nozzle.

1. When $P_0 > P_b > P_C$, the flow remains subsonic throughout the nozzle, and the mass flow is less than that for choked flow. The fluid velocity increases in the first (converging) section and reaches a maximum at the throat (but Ma < 1).

However, most of the gain in velocity is lost in the second (diverging) section of the nozzle, which acts as a diffuser. The pressure decreases in the converging section, reaches a minimum at the throat, and increases at the expense of velocity in the diverging section.

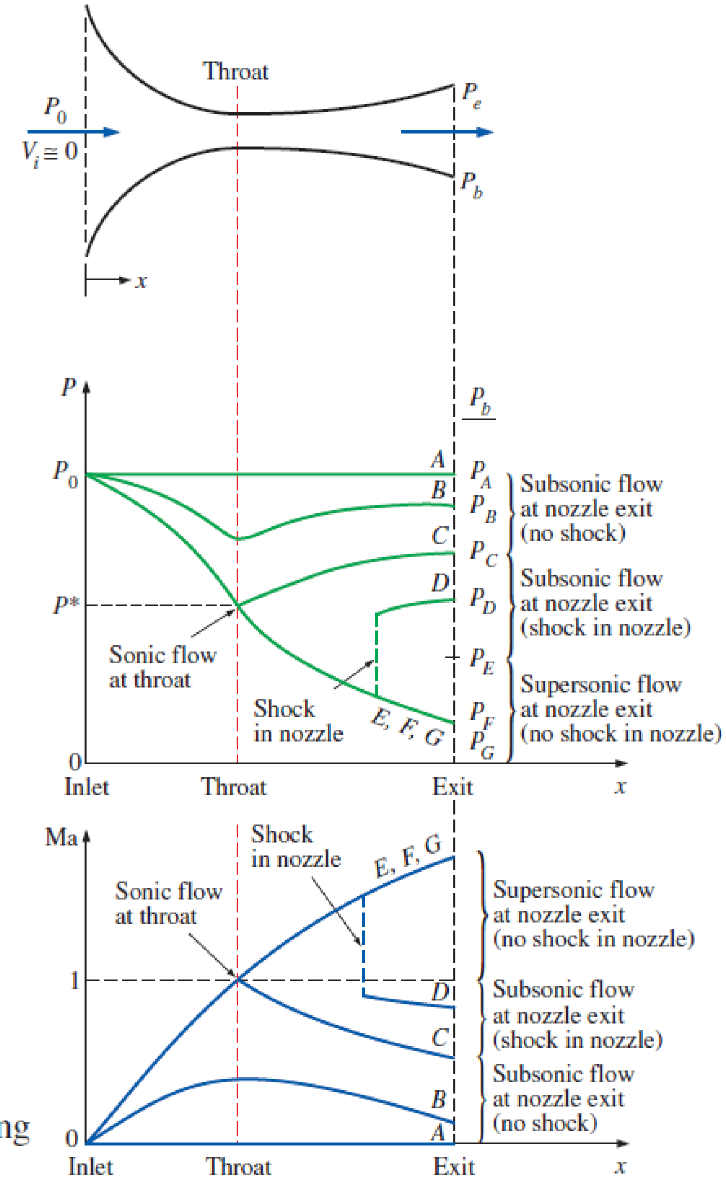

FIGURE 17–27
The effects of back pressure on the flow through a converging–diverging nozzle.

2. When $P_b = P_C$, the throat pressure becomes P^* and the fluid achieves sonic velocity at the throat. But the diverging section of the nozzle still acts as a diffuser, slowing the fluid to subsonic velocities. The mass flow rate that was increasing with decreasing P_b also reaches its maximum value.

3. When $P_C > P_b > P_E$, the fluid that achieved a sonic velocity at the throat continues accelerating to supersonic velocities in the diverging section as the pressure decreases. This acceleration comes to a sudden stop, however, as a **normal shock** develops at a section between the throat and the exit plane, which causes a sudden drop in velocity to subsonic levels and a sudden increase in pressure. The fluid then continues to decelerate further in the remaining part of the converging–diverging nozzle.

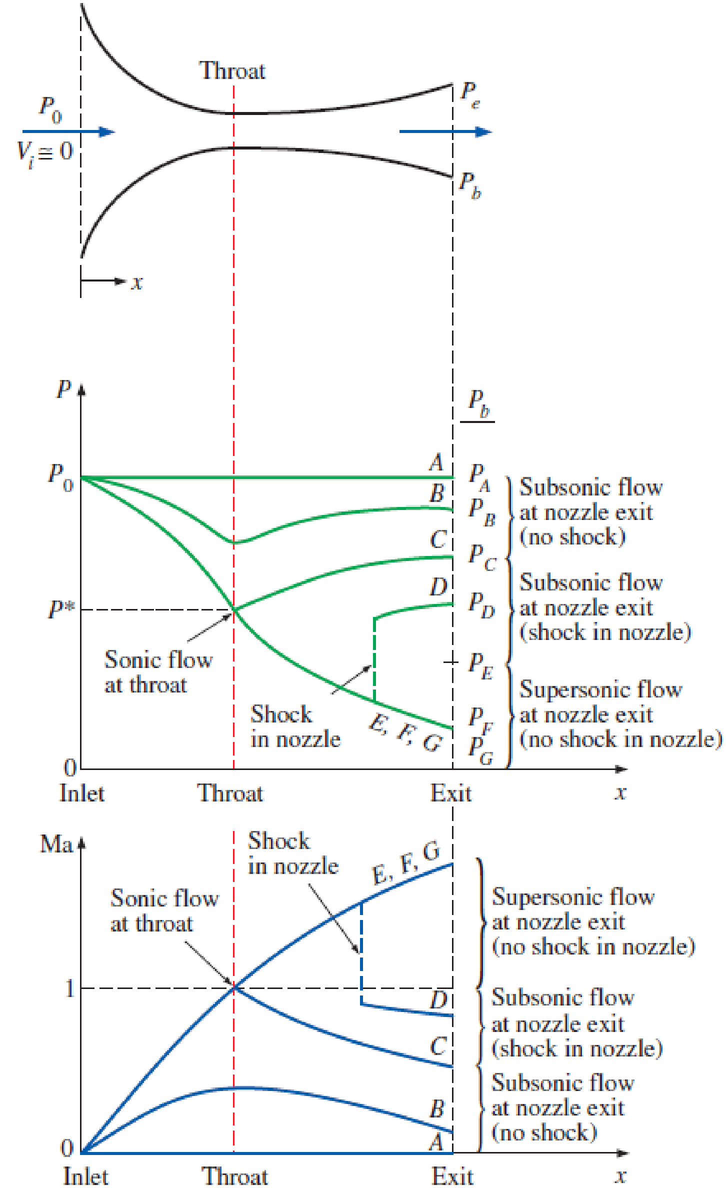

4. When $P_E > Pb > 0$, the flow in the diverging section is supersonic, and the fluid expands to P_F at the nozzle exit with no normal shock forming within the nozzle. Thus, the flow through the nozzle can be approximated as isentropic.

When $P_b = P_F$, no shocks occur within or outside the nozzle.

When $P_b < P_F$, irreversible mixing and expansion waves occur downstream of the exit plane of the nozzle.

When $P_b > P_F$, however, the pressure of the fluid increases from P_F to P_b irreversibly in the wake of the nozzle exit, creating what are called *oblique shocks.*

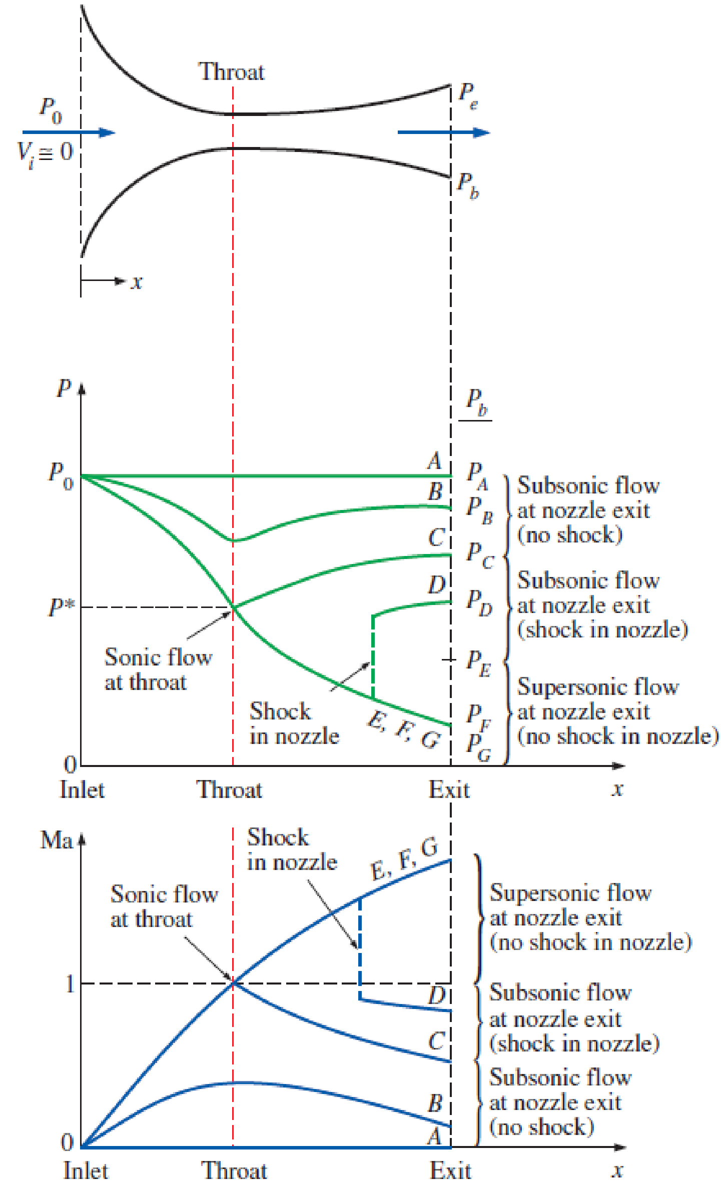

For some back pressure values, abrupt changes in fluid properties occur in a very thin section of a converging–diverging nozzle under supersonic flow conditions, creating a **shock wave**.

We study the conditions under which shock waves develop and how they affect the flow.

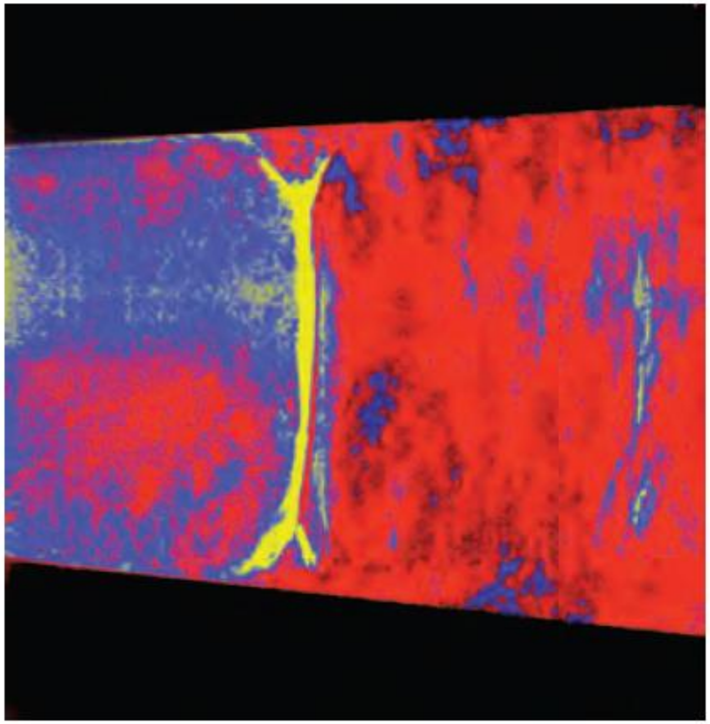

FIGURE 17–30
Schlieren image of a normal shock in a Laval nozzle. The Mach number in the nozzle just upstream (to the left) of the shock wave is about 1.3. Boundary layers distort the shape of the normal shock near the walls and lead to flow separation beneath the shock.

Normal Shocks

Normal shock waves: The shock waves that occur in a plane normal to the direction of flow. The flow process through the shock wave is highly irreversible.

Conservation of mass:

$$\rho_1 A V_1 = \rho_2 A V_2$$

$$\rho_1 V_1 = \rho_2 V_2$$

Conservation of energy:

$$h_1 + \frac{V_1^2}{2} = h_2 + \frac{V_2^2}{2}$$

$$h_{01} = h_{02}$$

Linear momentum equation:

$$A(P_1 - P_2) = \dot{m}(V_2 - V_1)$$

Increase of entropy: $s_2 - s_1 \geq 0$

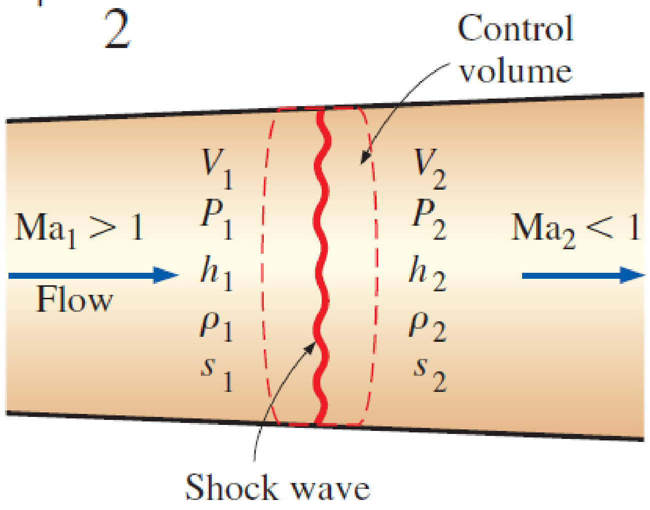

FIGURE 17–29
Control volume for flow across a normal shock wave.

Fanno line: Combining the conservation of mass and energy relations into a single equation and plotting it on an *h*-*s* diagram yield a curve. It is the locus of states that have the same value of stagnation enthalpy and mass flux.

Rayleigh line: Combining the conservation of mass and momentum equations into a single equation and plotting it on the *h*-*s* diagram yield a curve.

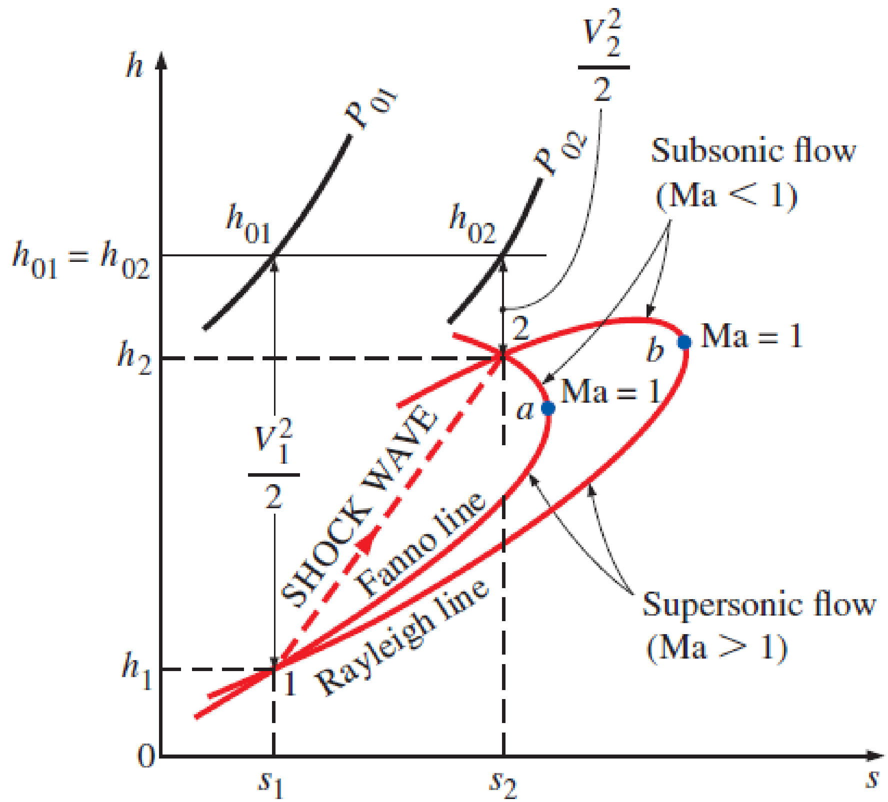

FIGURE 17–31
The *h*-*s* diagram for flow across a normal shock.

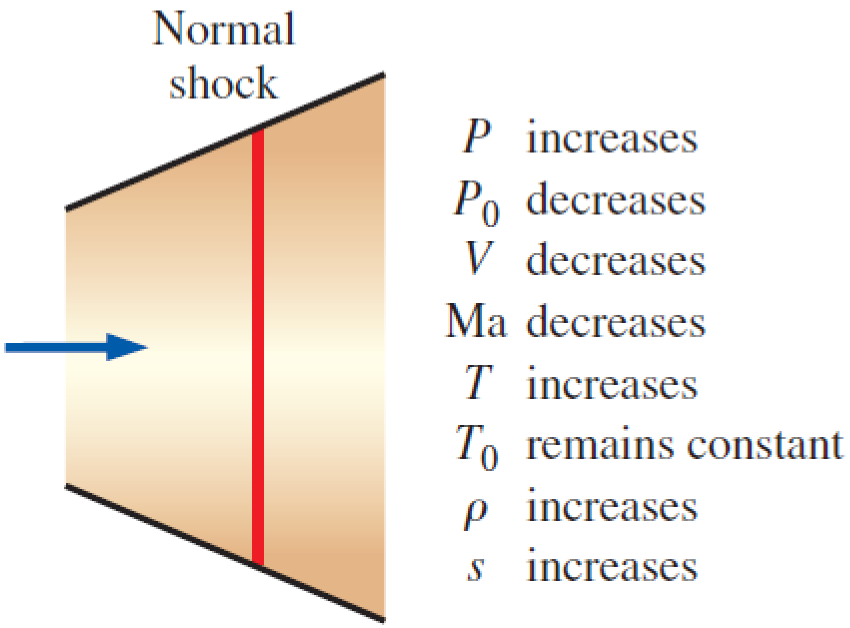

FIGURE 17–32

Variation of flow properties across a normal shock in an ideal gas.

The relations between various properties before and after the shock for an ideal gas with constant specific heats:

$$\frac{T_2}{T_1} = \frac{P_2 V_2}{P_1 V_1} = \frac{P_2 \mathrm{Ma}_2 c_2}{P_1 \mathrm{Ma}_1 c_1} = \frac{P_2 \mathrm{Ma}_2 \sqrt{T_2}}{P_1 \mathrm{Ma}_1 \sqrt{T_1}} = \left(\frac{P_2}{P_1}\right)^2 \left(\frac{\mathrm{Ma}_2}{\mathrm{Ma}_1}\right)^2$$

Fanno line: $$\frac{P_2}{P_1} = \frac{\mathrm{Ma}_1 \sqrt{1 + \mathrm{Ma}_1^2 (k-1)/2}}{\mathrm{Ma}_2 \sqrt{1 + \mathrm{Ma}_2^2 (k-1)/2}}$$

Rayleigh line: $$\frac{P_2}{P_1} = \frac{1 + k\mathrm{Ma}_1^2}{1 + k\mathrm{Ma}_2^2}$$

$$\mathrm{Ma}_2^2 = \frac{\mathrm{Ma}_1^2 + 2/(k-1)}{2\mathrm{Ma}_1^2 k/(k-1) - 1}$$

This represents the intersections of the Fanno and Rayleigh lines and relates the Mach number upstream of the shock to that downstream of the shock.

Various flow property ratios across the shock are listed in Table A–33.

FIGURE 17–33
The air inlet of a supersonic fighter jet is designed such that a shock wave at the inlet decelerates the air to subsonic velocities, increasing the pressure and temperature of the air before it enters the engine.

17-5. SHOCK WAVES AND EXPANSION WAVES

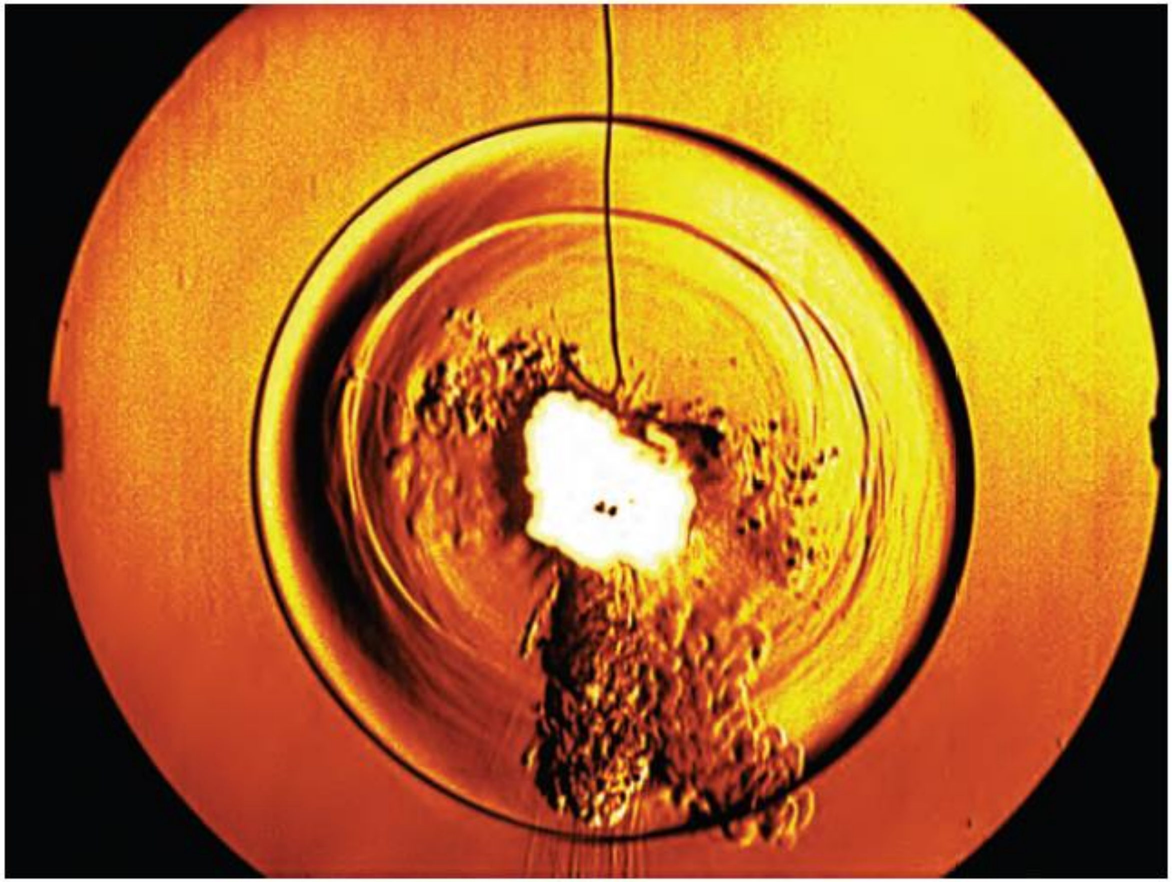

FIGURE 17–34
Schlieren image of the blast wave (expanding spherical normal shock) produced by the explosion of a firecracker. The shock expanded radially outward in all directions at a supersonic speed that decreased with radius from the center of the explosion. A microphone sensed the sudden change in pressure of the passing shock wave and triggered the microsecond flashlamp that exposed the photograph.

G.S. Settles, Gas Dynamics Lab, Penn State University. Used with permission

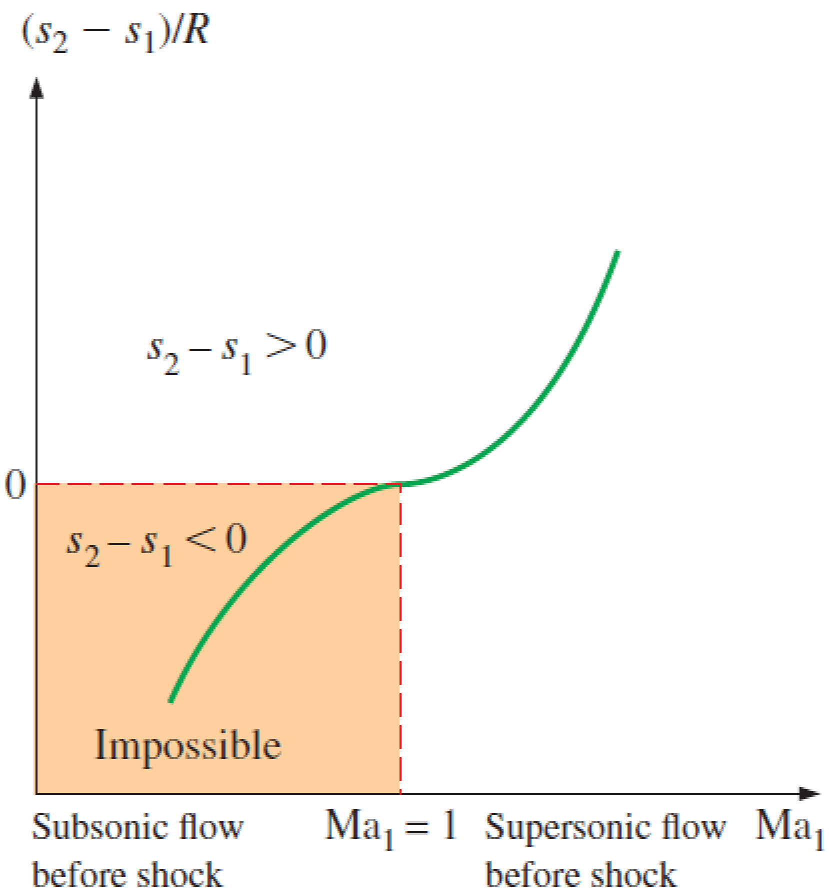

FIGURE 17–35
Entropy change across a normal shock.

$$s_2 - s_1 = c_p \ln \frac{T_2}{T_1} - R \ln \frac{P_2}{P_1}$$

Since the flow across the shock is adiabatic and irreversible, the second law requires that the entropy increase across the shock wave.

Thus, a shock wave cannot exist for values of Ma_1 less than unity where the entropy change would be negative.

For adiabatic flows, shock waves can exist only for supersonic flows, $Ma_1 > 1$.

FIGURE 17–37

When a lion tamer cracks his whip, a weak spherical shock wave forms near the tip and spreads out radially; the pressure inside the expanding shock wave is higher than ambient air pressure, and this is what causes the crack when the shock wave reaches the lion's ear.

Oblique Shocks

When the space shuttle travels at supersonic speeds through the atmosphere, it produces a complicated shock pattern consisting of inclined shock waves called **oblique shocks**.

Some portions of an oblique shock are curved, while other portions are straight.

FIGURE 17–38
Schlieren image of a small model of the space shuttle orbiter being tested at Mach 3 in the supersonic wind tunnel of the Penn State Gas Dynamics Lab. Several *oblique shocks* are seen in the air surrounding the spacecraft.
G.S. Settles, Gas Dynamics Lab, Penn State University. Used with permission

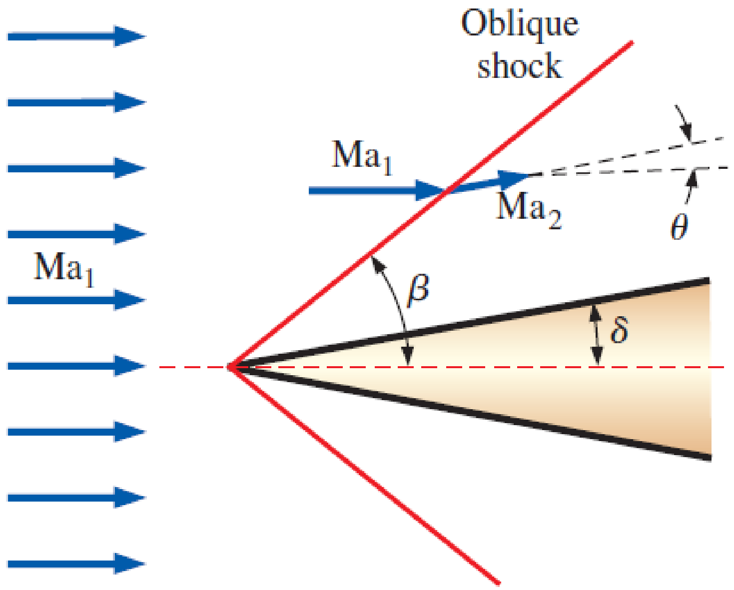

FIGURE 17–39

An oblique shock of *shock angle* β formed by a slender, two-dimensional wedge of half-angle δ. The flow is turned by *deflection angle* θ downstream of the shock, and the Mach number decreases.

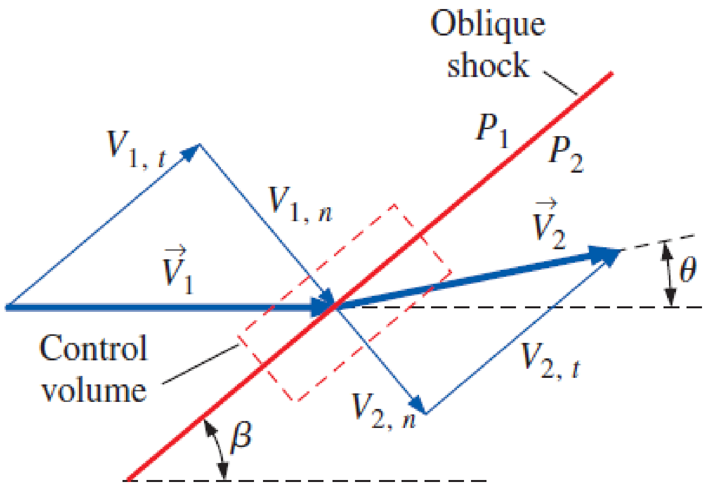

FIGURE 17–40

Velocity vectors through an oblique shock of shock angle β and deflection angle θ.

Unlike normal shocks, in which the downstream Mach number is always subsonic, Ma_2 downstream of an oblique shock can be subsonic, sonic, or supersonic, depending on the upstream Mach number Ma_1 and the turning angle.

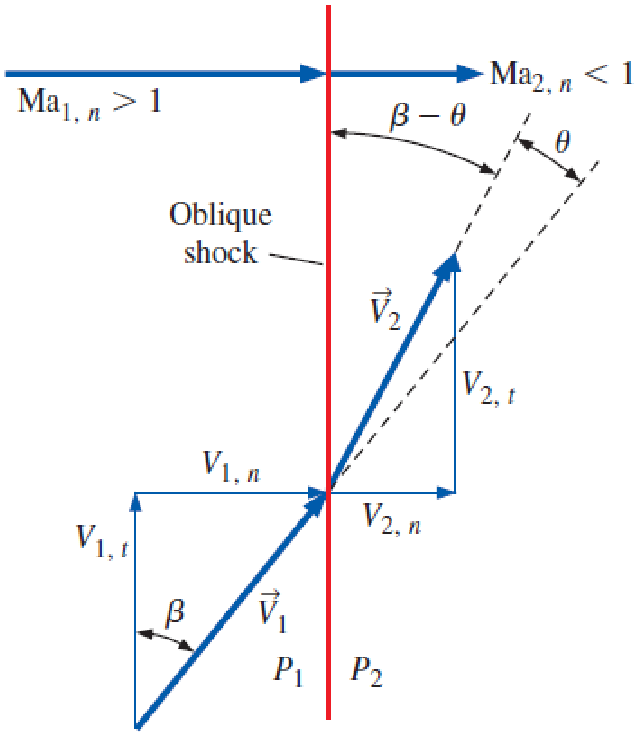

FIGURE 17–41
The same velocity vectors of Fig. 17–40, but rotated by angle $\pi/2 - \beta$, so that the oblique shock is vertical. Normal Mach numbers $Ma_{1,n}$ and $Ma_{2,n}$ are also defined.

$$h_{01} = h_{02} \quad \rightarrow \quad T_{01} = T_{02}$$

$$Ma_{2,n} = \sqrt{\frac{(k-1)Ma_{1,n}^2 + 2}{2k Ma_{1,n}^2 - k + 1}}$$

$$\frac{P_2}{P_1} = \frac{2k\, Ma_{1,n}^2 - k + 1}{k+1}$$

$$\frac{\rho_2}{\rho_1} = \frac{V_{1,n}}{V_{2,n}} = \frac{(k+1)Ma_{1,n}^2}{2 + (k-1)Ma_{1,n}^2}$$

$$\frac{T_2}{T_1} = [2 + (k-1)Ma_{1,n}^2]\frac{2k\, Ma_{1,n}^2 - k + 1}{(k+1)^2 Ma_{1,n}^2}$$

$$\frac{P_{02}}{P_{01}} = \left[\frac{(k+1)Ma_{1,n}^2}{2 + (k-1)Ma_{1,n}^2}\right]^{k/(k-1)} \left[\frac{(k+1)}{2k\, Ma_{1,n}^2 - k + 1}\right]^{1/(k-1)}$$

FIGURE 17–42
Relationships across an oblique shock for an ideal gas in terms of the normal component of upstream Mach number $Ma_{1,n}$.

All the equations, shock tables, etc., for normal shocks apply to oblique shocks as well, provided that we use only the **normal** components of the Mach number.

17-5. SHOCK WAVES AND EXPANSION WAVES

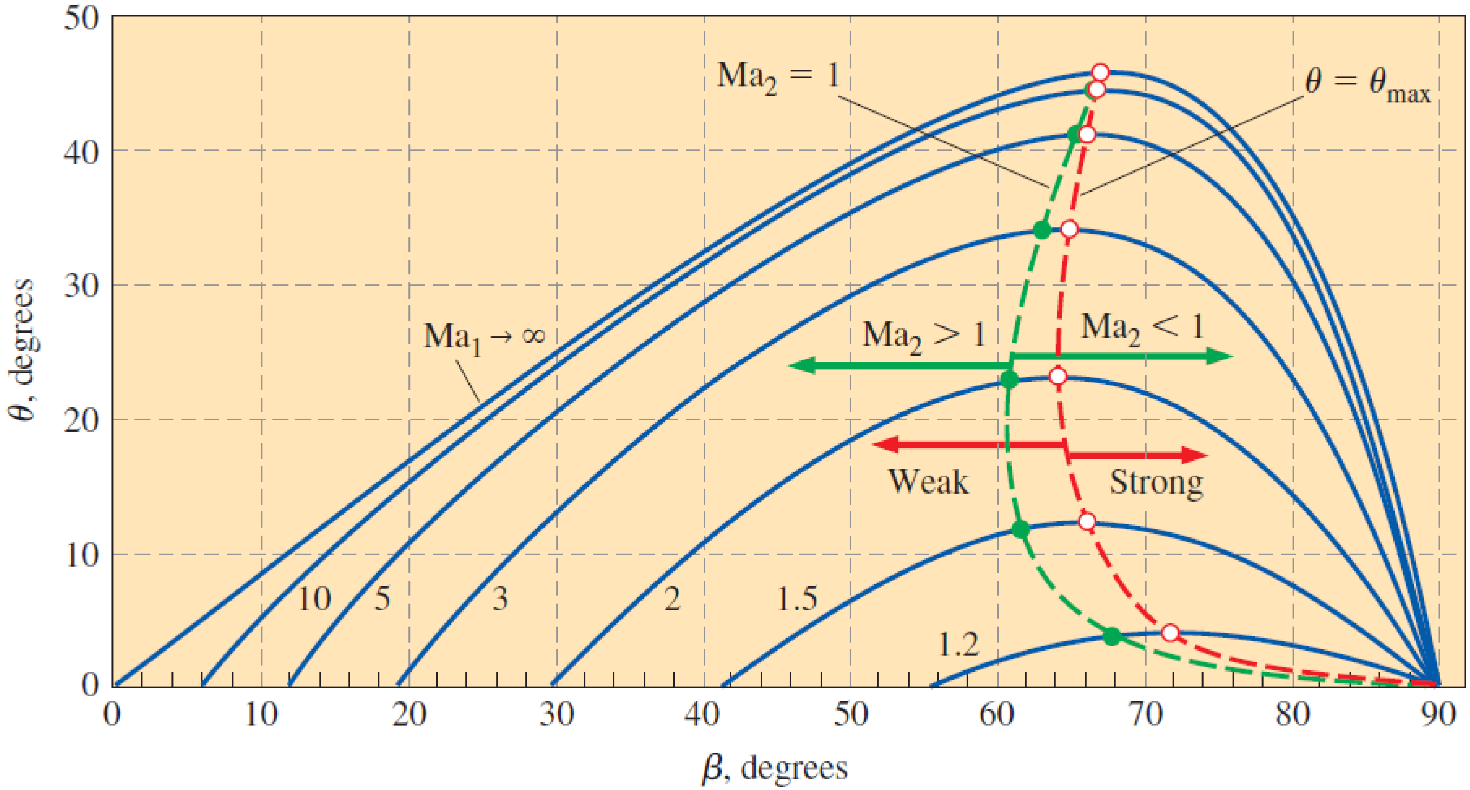

The dependence of straight oblique shock deflection angle θ on shock angle β for several values of upstream Mach number Ma_1. Calculations are for an ideal gas with $k = 1.4$. The dashed black line connects points of maximum deflection angle ($\theta = \theta_{max}$). *Weak oblique shocks* are to the left of this line, while *strong oblique shocks* are to the right of this line. The dashed gray line connects points where the downstream Mach number is *sonic* ($Ma_2 = 1$). *Supersonic downstream flow* ($Ma_2 > 1$) is to the left of this line, while *subsonic downstream flow* ($Ma_2 < 1$) is to the right of this line.

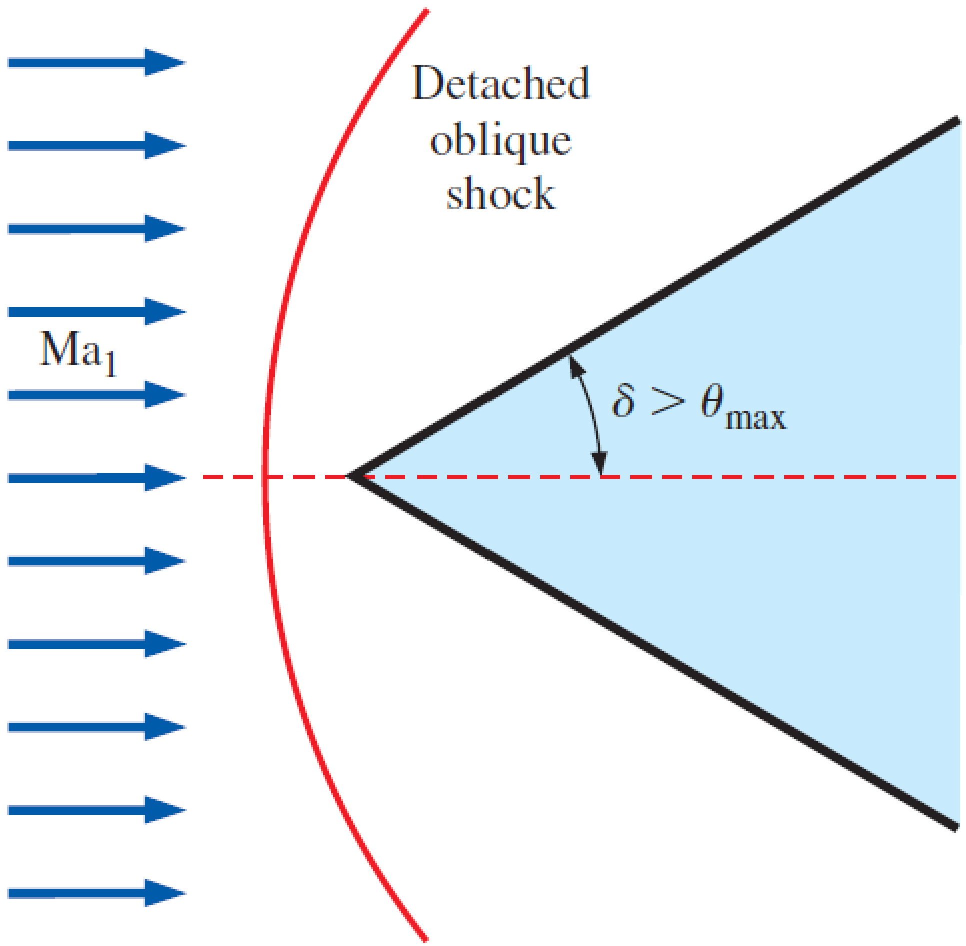

FIGURE 17–44

A *detached oblique shock* occurs upstream of a two-dimensional wedge of half-angle δ when δ is greater than the maximum possible deflection angle θ. A shock of this kind is called a *bow wave* because of its resemblance to the water wave that forms at the bow of a ship.

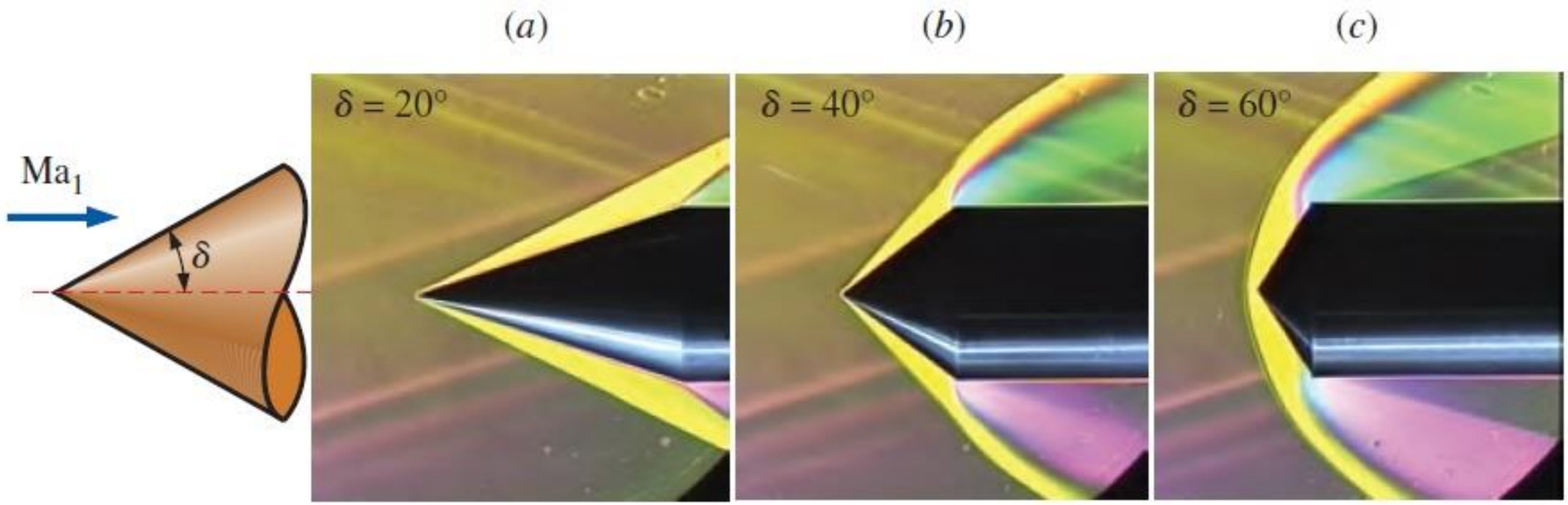

FIGURE 17–45
Still frames from schlieren videography illustrating the detachment of an oblique shock from a cone with increasing cone half-angle δ in air at Mach 3. At (*a*) $\delta = 20°$ and (*b*) $\delta = 40°$, the oblique shock remains attached, but by (*c*) $\delta = 60°$, the oblique shock has detached, forming a bow wave.

Mach angle

$$\mu = \sin^{-1}(1/\mathrm{Ma}_1)$$

FIGURE 17–46
Color schlieren image of Mach 3.0 flow from left to right over a sphere. A curved shock wave called a *bow shock* forms in front of the sphere and curves downstream.

Prandtl–Meyer Expansion Waves

We now address situations where supersonic flow is turned in the *opposite* direction, such as in the upper portion of a two-dimensional wedge at an angle of attack greater than its half-angle δ.

We refer to this type of flow as an **expanding flow**, whereas a flow that produces an oblique shock may be called a **compressing flow**.

As previously, the flow changes direction to conserve mass. However, unlike a compressing flow, an expanding flow does *not* result in a shock wave.

Rather, a continuous expanding region called an **expansion fan** appears, composed of an infinite number of Mach waves called **Prandtl–Meyer expansion waves**.

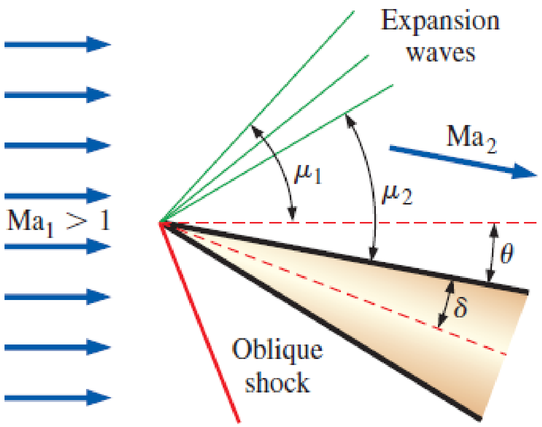

FIGURE 17–47
An expansion fan in the upper portion of the flow formed by a two-dimensional wedge at an angle of attack in a supersonic flow. The flow is turned by angle θ, and the Mach number increases across the expansion fan. Mach angles upstream and downstream of the expansion fan are indicated. Only three expansion waves are shown for simplicity, but in fact, there are an infinite number of them. (An oblique shock is also present in the bottom portion of this flow.)

Turning angle across an expansion fan: $\theta = \nu(\mathrm{Ma}_2) - \nu(\mathrm{Ma}_1)$

Prandtl–Meyer function

$$\nu(\mathrm{Ma}) = \sqrt{\frac{k+1}{k-1}}\tan^{-1}\left(\sqrt{\frac{k-1}{k+1}(\mathrm{Ma}^2-1)}\right) - \tan^{-1}\left(\sqrt{\mathrm{Ma}^2-1}\right)$$

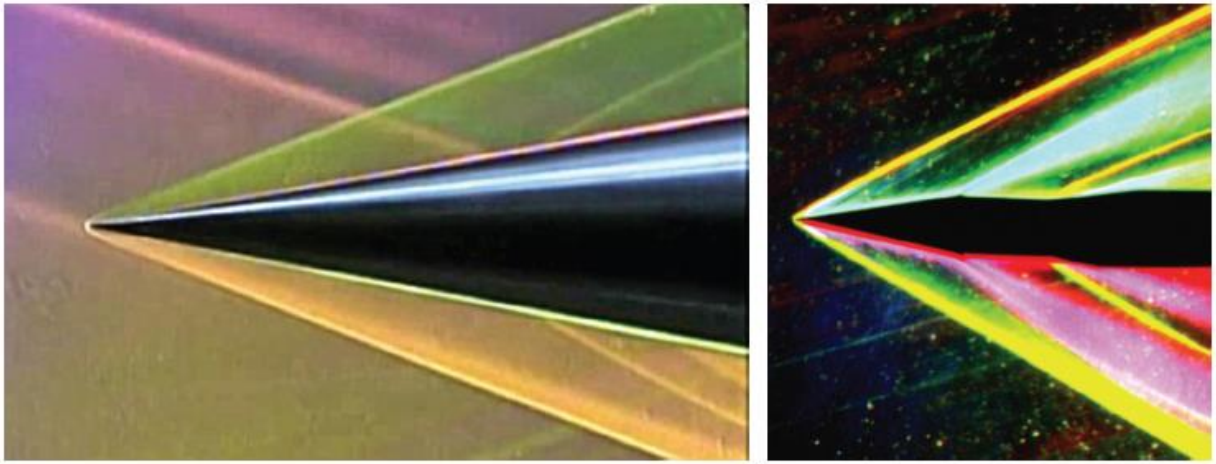

(*a*) (*b*)

FIGURE 17–48

(*a*) Mach 3 flow over an axisymmetric cone of 10° half-angle. The boundary layer becomes turbulent shortly downstream of the nose, generating Mach waves that are visible in the color schlieren image. (*b*) A similar pattern is seen in this color schlieren image for Mach 3 flow over an 11° 2-D wedge. Expansion waves are seen at the corners where the wedge flattens out.

(a) and (b): ©G. S. Settles, Gas Dynamics Lab, Penn State University. Used with permission

17-5. SHOCK WAVES AND EXPANSION WAVES

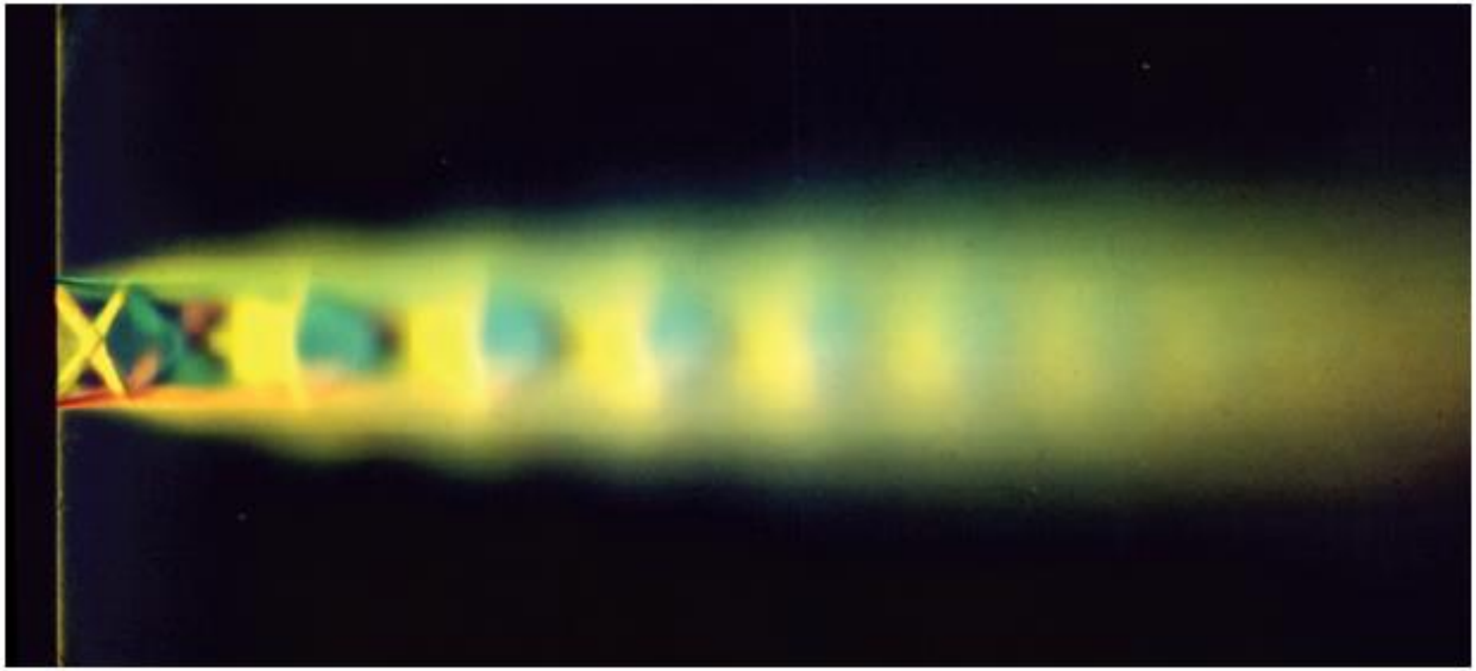

FIGURE 17–49
The complex interactions between shock waves and expansion waves in an "overexpanded" supersonic jet.

Summary

- Stagnation properties
- Speed of sound and Mach number
- One-dimensional isentropic flow
- Isentropic flow through nozzles
- Shock waves and expansion waves
- Duct flow with heat transfer and negligible friction (Rayleigh flow)
- Steam nozzles